# Mechanical, Chemical, and Physical Properties of Wood and Perennial Grass Biochars for Possible Composite Application

Ehsan Behazin,[a] Emmanuel Ogunsona,[a] Arturo Rodriguez-Uribe,[b] Amar K. Mohanty,[a,b,*] Manjusri Misra,[a,b] and Anthony O. Anyia [c]

Miscanthus, switchgrass, and softwood chip biochars, produced by slow pyrolysis, were characterized to evaluate their properties in light of potential alternative and novel applications. This work investigated specific physical and chemical properties of biochars that have not been previously reported. Atomic force microscopy (AFM), moisture absorption, and electrical and thermal analysis were conducted to demonstrate the mechanical, physical, and chemical properties of biochars. In addition, elemental analysis, specific surface area, Fourier transform infrared in the attenuated total reflectance (FTIR-ATR), and X-ray diffraction were performed. The state-of-art quantitative nano-mechanical measurement yielded a modulus of elasticity of approximately 10 GPa for the wood chip biochar, while the grass-based samples exhibited a comparatively lower modulus of approximately 5 GPa. In addition, the pore blocking phenomenon by water molecules was identified as a cause for atypical behavior of the biochars' moisture absorptions, resulting in wood chip biochar having the lowest equilibrium moisture content of 6.2 wt.%. Results from electrical and thermal conductivity measurements demonstrated relatively lower values in comparison to carbonized biomass.

*Keywords: Biochar; Slow pyrolysis; BET surface analysis; Atomic force microscopy; Elemental analysis*

*Contact information: a: School of Engineering, Thornbrough Building, University of Guelph, 50 Stone Road East, Guelph, ON N1G 2W1, Canada; b: Bioproducts Discovery & Development Centre, Department of Plant Agriculture, Crop Science Building, University of Guelph, 50 Stone Road East, Guelph, ON N1G 2W1, Canada; c: Bioresource Technologies, Alberta Innovates-Technology Futures, Vegreville, Alberta, T9C 1T4, Canada; *Corresponding author: mohanty@uoguelph.ca*

## INTRODUCTION

While society's dependence on fossil fuels is at its peak, petroleum resources are fast diminishing. Petroleum-based derivatives, such as energy in the form of gas to heat homes and gasoline/diesel to fuel vehicles, and materials such as plastics, are being consumed at an alarming rate. In order to reduce the consumption and dependence on petroleum-based derivatives, alternatives have to be explored and implemented (Cherubini 2010).

Shifting to more sustainable alternatives has created an increasing interest in obtaining fuels and chemicals from bioresources. Two major pathways for the conversion of biomass to bio-fuels involve biochemical and thermochemical treatments. These treatments have attracted commercial interest and have moved on to the commercialization level thanks to biorefinery infrastructure. The thermochemical pathway has the advantage of using the entire biomass feedstock over the biochemical pathway, which mainly

consumes delignified products. Also, the use of agricultural and forestry materials, industrial co-products (lignin), and clean municipal disposal waste in thermochemical processes has been an effective way to manage waste (Lehmann and Joseph 2009). Pyrolysis is a well-known thermochemical process in which the thermal degradation of biomass is performed at elevated temperatures in an oxygen-controlled atmosphere. Pyrolysis at temperatures between 200 to 350 °C is known as torrefaction (Tumuluru *et al.* 2012). On the other hand, high temperature pyrolysis normally used for production of bio-fuels and performed at temperatures higher than 500 °C (Gaskin *et al.* 2008). By means of pyrolysis, biomass having relatively low density and energy can be converted to higher density and/or energy products, such as bio-oil, bio-char, and syngas (Laird *et al.* 2009). Different pyrolysis systems—known as slow, intermediate, and flash—have been devised for producing these products (Shackley *et al.* 2013). Biochars are produced as the byproducts from fast pyrolysis or as the main product of slow pyrolysis of biomass.

Typically, fast pyrolysis produces around 50 to 70% of bio-oil and 10 to 25% of biochar, while in the slow pyrolysis process, higher biochar yields of 25 to 35% are reported in the literature (Shackley *et al.* 2013). Considering the low value of biochar when used as carbon sequestration credit (Brown *et al.* 2011), the viability and sustainability of both pyrolysis processes, especially slow pyrolysis would be compromised. Finding a value-added alternative for biochar such as composites applications (Mohanty *et al.* 2015) would considerably support the sustainability of such systems in the future.

Evidence shows the possible presence of toxic elements such as polycyclic aromatic hydrocarbons (PAHs) in biochar (Freddo *et al.* 2012). Therefore, discovering applications for biochar for which PAHs are not of concern would broaden its utilization scope.

Characterization of biochar produces fundamental knowledge about the diverse properties of different biochar for its use in different applications. For example, biochars derived from fast pyrolysis present basic chemical and physical differences compared to those produced by slow pyrolysis. These differences may be related to the origin of the biomass and/or may be attributed to variations in the processing method. Most commercial biochar products are produced either from wood scraps or perennial grasses. However, a variety of materials can be used, such as industrial and municipal wastes (Van Zwieten *et al.* 2009). The chemical and physical characteristics of biochars produced from fast or slow pyrolysis exhibit changes in the elemental concentrations of C, H, N, S, O, and ash, as well as in their porosity. Until now, major works in the characterization of biochar have focused on the properties involved in the enhancement of soil fertility. Warnock *et al.* (2007) studied the effect of mycorrhizae on biochar in relation to soil enhancement. Asai *et al.* (2009) investigated the effect of biochar application into the soil on the growth and production of rice. Atkinson *et al.* (2010) reviewed the mechanisms and effects of biochar on temperate soils. Spokas *et al.* (2009) looked at the sorption properties of greenhouse gasses and the degradation of herbicides when biochar is added to soil. More recently, Khan *et al.* (2015) evaluated properties of thermomechanical pulp sludge biochar as a growth media for greenhouse vegetables.

Recently, many researchers have attempted to discover new applications for biochar targeting applications other than soil enhancement. Work done by Yu *et al.* (2011) focused on the catalytic properties of biochar for the transesterification of canola oil. Koutcheiko and Vorontsov (2013) researched biochar derived from wood to be utilized as supercapitors. The utilization of biochar as a reinforcement in rubber (Peterson 2012), water filtration media (Peterson *et al.* 2012), and phosphate removal additive (Yao *et al.* 2013) have been investigated. Other applications of biochar, such as enzyme

immobilization (González *et al.* 2013) and as an asphalt flow modifier (Walters *et al.* 2014) have also been investigated. Emerging applications in biochar utilization require more knowledge about the general properties of biochar. Fundamental research in this area would provide a proper platform for the value-added utilization of co-products from thermochemical processes (biochar specifically) through product diversification. This would in turn provide a more sustainable bio-economy.

In this study, new properties of biochar were investigated to evaluate the use of biochar for different applications. Properties, such as modulus of elasticity, electrical and thermal conductivity, moisture absorption, elemental compositions, surface area, functional groups, and others were investigated. These properties were measured to generate essential information needed for developing potential value-added applications for biochar.

## EXPERIMENTAL

The biochars used in this study were miscanthus (MB), switchgrass (SB), (Genesis Industries, CA, USA), and softwood chip biochar (WCB) (Alberta Innovates Technology Futures, AB, Canada). All biochars were produced by slow pyrolysis at an average pyrolysis temperature of 500 °C.

All samples were ball-milled for 1 h at 300 rpm. The rotation direction was changed after 30 min of milling. Each biochar sample was weighed to approximately 38 g and put in a 500 mL stainless steel ball mill container. A hardened steel ball with a 40 mm diameter was used (weight ratio of ball to biochar was 7:1). Biochar was sieved using a sieve shaker to obtain a particle size ranging from 297 to 300 µm. These were used in the surface area measurement, thermal and electrical conductivity tests, and moisture absorption analysis. A similar particle size was used to reduce or eliminate the possible effects that different particle size ranges could have on the above mentioned test results.

The elements present and their compositions were determined using a Flash 2000 CHNS/O Elemental Analyzer (Thermo Fisher Scientific Inc., Waltham, MA, USA) with three replicates for each condition. The ash content was determined by heating the samples in a muffle furnace according to ASTM D1762-84 (2013). Thermogravimetric analyses (TGA) were carried out on milled samples in a thermogravimetric analyzer (TA Q400, TA Instruments, USA). These tests studied the weight loss profile in a two-step process starting with a nitrogen atmosphere and then switching to a pure oxygen environment. Volatile matter and fixed carbon content were measured according to ASTM E1131-08 (2014). The heating rate was fixed at 20 °C/min and gas was switched over at 900 °C.

The surface analysis was performed on a Quantachrome Nova 2000 series (Quantachrome Instruments, USA). Prior to testing, the sieved samples were degassed under a vacuum for 8 h at 105 °C. The surface analysis tests were carried out using the Brunauer-Emmett-Teller (BET) multi-point method at -196 °C with nitrogen gas at a relative pressures ($P/P_o$) ranging from 0.25 to 0.30. The pore size distribution was obtained by applying quenched solid density function theory (QSDFT) method to $N_2$ adsorption data assuming cylindrical pores. At least three replicates were used for obtaining the average values.

Scanning electron micrographs of the samples were taken using a Phenom Pro X (PhenomWorld, Netherlands) at an acceleration voltage of 10 kV. Superficial elemental

carbon and oxygen of biochars was performed using the incorporated spectroscopy technique of energy dispersion (EDS).

Powders of the biochars were pressed flat against the diamond crystal surface of a Fourier transform infrared-attenuated total reflectance (FTIR-ATR) instrument (Nicolet 6700, Thermo Fisher Scientific, USA). The absorbance was measured from 4000 to 400 $cm^{-1}$ using 32 scans per sample and a resolution of 4 $cm^{-1}$. The spectra were corrected using the surrounding air as the background spectrum. The results were analyzed using OMNIC Spectra software (Thermo Fisher Scientific).

Moisture absorption of the samples was measured using an environmental chamber (Endurance® Series C340, Envirotronics, USA). The sieved samples were kept at 50% relative humidity and 21 °C, and weight changes were measured every 2 h for the first 10 h and every 24 h thereafter. All samples were measured in duplicates.

The thermal conductivity of the different biochars was performed using a unit TPS 500 (ThermTest, Inc., Canada). A Kapton disc-type sensor, with a diameter of 6.378 mm, was placed between the powdery biochars and held in place by the sample holder. Three experiments were conducted per sample. The conditions of each experiment were 250 mW, 10 sec, and 60 Hz.

The electrical conductivities were measured using an Autolab PGSTAT302N (Metrihm Autolab BV, Netherlands) installed with a module FRA32 M for impedance. The frequency range was 400 to 600 Hz at a sine wave amplitude of 10 mV. The test was performed at room temperature (23 °C). Small amounts of each sample (0.3 g) were placed in a cylindrical groove featuring a 10 mm inside diameter and then compressed at 12 KPa (using the weight of the upper piston between the two aluminum pistons). Data were acquired using Nova 1.8.17 software (Quantachrome Instruments, USA).

Fifty grams of dried milled biochar was sieved into various particle sizes using a sieve shaker for 10 min. The weight of the sieve before and after sieving was recorded, and the difference was recorded as the weight fraction of the particle size distribution of the biochar.

X-ray diffraction (XRD) measurements were recorded using a Powder Diffractometer (Stoe & Cie GmbH, Germany) with an Enraf Nonius F571 Cu rotating anode using the Kalpha1 and Kalpha2 wavelengths. A Moxcet solid state detector was used, and the rotating anode was run at 40 keV and 20 mA.

Biochar Derjaguin-Muller-Toporov (DMT) elastic moduli were measured using a Nanoscope Multimode 8 (Bruker, USA) featuring a NanoScope V controller and NanoScope version 8.10 software. Image processing and data analysis were performed with the NanoScope Analysis software version 1.50. Peak force quantitative nano-mechanical (PFQNM) mode, with a high-sensitivity silicon probe known as a TAP500a, was used to scan the samples. Samples were prepared by embedding biochars in a polypropylene (PP) matrix at 40 wt. % loading. All samples were microtomed (Leica Ultracut, Leica, Wetzlar, Germany) to obtain very flat surfaces for atomic force microscopy (AFM) analysis. The cantilever was calibrated using a polystyrene-based film (PS) reference standard, provided by the Bruker Company (Santa Barbara, CA, USA), before the DMT modulus was determined. As a result, the tip radius was estimated at 15.3 nm, with a spring constant of 70 N/m. The average deformation on the reference PS film was captured through the deformation channel (2.84 nm). The modulus measurement of force set points was changed in order to produce the same amount of deformation on the biochar's surface.

## RESULTS AND DISCUSSION

The elemental composition, surface, and EDS analysis results for all biochars are listed in Table 1. No traces of sulfur were detected in any of the biochar samples. The highest and lowest amounts of ash were found in switchgrass and wood chip biochars, respectively. Nitrogen was found to be higher in miscanthus and switchgrass (grass-based samples) compared to wood samples, which is consistent with the fact the nitrogen is more abundant in grasses than woods (Caillat and Vakkilainen 2013). The amount of ash in switchgrass and miscanthus was consistent with the results obtained by Tanger *et al.* (2013).

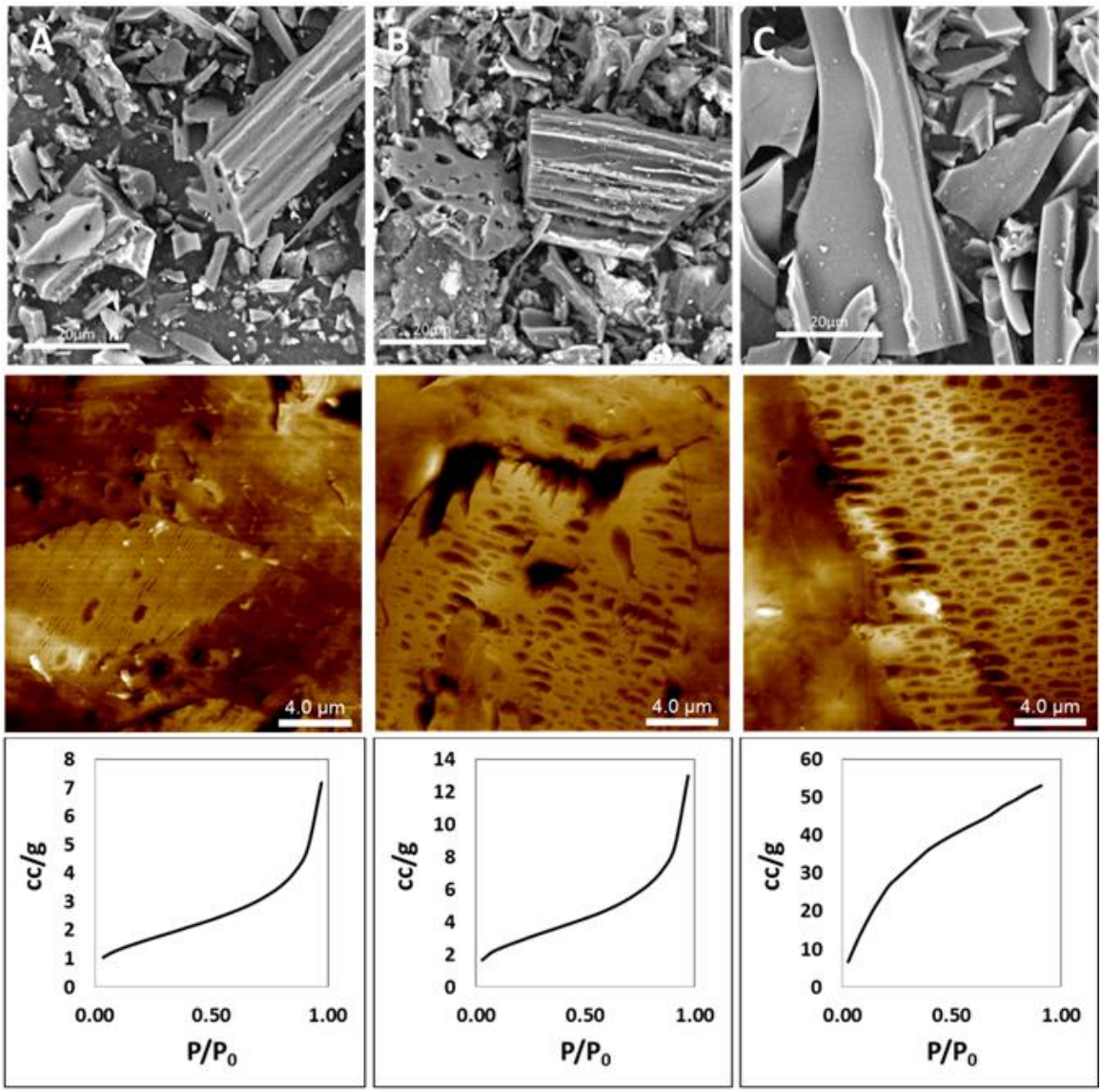


**Fig. 1.** Top - Micrographs of (A) Miscanthus biochar, (B) Switchgrass biochar, and (C) Wood chip biochar. Middle - AFM height images of microtomed biochars embedded in the PP matrix. Bottom - Nitrogen adsorption isotherm for corresponding biochars

**Table 1.** Elemental Composition, Atomic Ratio, Fixed Carbon, Volatile Matter, and BET $N_2$ Surface Area of Biochars

| | Component, wt.% | | | | | | | Atomic Ratio [a] | | SA | Total pore volume | EDS | | |
|---|---|---|---|---|---|---|---|---|---|---|---|---|---|---|
| Sample | C (%) | H (%) | N (%) | O (%) | Ash (%) | Fixed carbon (%) | Volatile matter (%) | H/C | O/C | ($m^2$/g) | (cc/g) [$10^{-2}$] | C (%) | O (%) | O/C |
| MB | 66.49 (0.38) | 2.90 (0.07) | 1.59 (0.34) | 22.88 (0.51) | 8.4 (0.03) | 58.04 (0.25) | 30.81 (0.29) | 0.52 | 0.26 | 6.52 (0.96) | 1.23 (0.18) | 67.6 (0.80) | 31.0 (0.85) | 0.34 |
| SB | 59.16 (0.25) | 2.37 (0.08) | 1.10 (0.09) | 18.95 (0.07) | 19.4 (0.03) | 48.32 (0.54) | 27.75 (0.28) | 0.48 | 0.24 | 10.26 (0.39) | 2.12 (0.16) | 64.8 (2.23) | 31.0 (0.85) | 0.36 |
| WCB | 81.01 (2.45) | 2.40 (0.13) | 0.50 (0.15) | 11.15 (0.62) | 1.3 (0.70) | 75.24 (0.76) | 18.72 (0.43) | 0.36 | 0.10 | 103.5 (1.64) | 7.76 (0.61) | 81.6 (0.30) | 18.4 (0.30) | 0.17 |

[a] Atomic ratios are calculated from CHNS/O results
Standard deviations are in parenthesis (at least three replicates were tested)

The atomic ratios of Oxygen/Carbon (O/C) obtained from the EDS analysis were used to compare the abundance of oxygenated groups on the surface of the biochars (Lee *et al.* 2010). The comparison of these ratios revealed that there were double the amount of oxygenated groups existing on the surface of MB and SB than on WCB.

The surface area of the WCB was approximately 10 times that of SB and 15 times that of MB. This result was further discussed in relation to the moisture adsorption and morphology. The SEM micrographs of the biochars (Fig. 1) show the MB and SB having porous structures with many grooves, while the WCB does not seem to have any visible pores at this scale. However, WCB exhibited the highest surface area from the BET results (Table 1), suggesting that the porosity was in a very small scale, which could not be visualized using SEM. On the other hand, the AFM height images of the microtomed biochars demonstrated a large difference in the porosity between samples. This was also confirmed through the shape of the adsorption isotherm curve, which tended to reach saturation as $P/P_0$ approaching one (Lowell *et al.* 2004).

The FTIR spectra of the MB and SB showed a more pronounced peak at 3400 $cm^{-1}$, which corresponds to the hydroxyl groups (Stuart 2004), while being almost flat in the spectrum of the WCB (Fig. 2). According to the results from the elemental analysis, MB and SB exhibited the highest O/C ratios, which is consistent with the less pronounced peak of WCB. The SB exhibited a distinct peak at 1080 $cm^{-1}$. This peak corresponds to the C-O stretching from carbohydrates (Schwanninger *et al.* 2004). The presence of carbohydrates may also explain the moisture uptake of SB compared to the other samples, as carbohydrates are hydrophilic because of the saturation with OH groups. The presence of several peaks common to all biochars was observed from the FTIR spectra. One such peak, arising at 2920 $cm^{-1}$, was related to the aliphatic C-H stretching vibration (Sarmah *et al.* 2010). The stretching vibration by the carbonyl groups of the carboxyl groups can be related to the peak at 1700 $cm^{-1}$ (Tatzber *et al.* 2007). The C=O stretching and aromatic C=C vibrations were attributed to the peak at 1580 $cm^{-1}$ (Smidt and Meissl 2007).

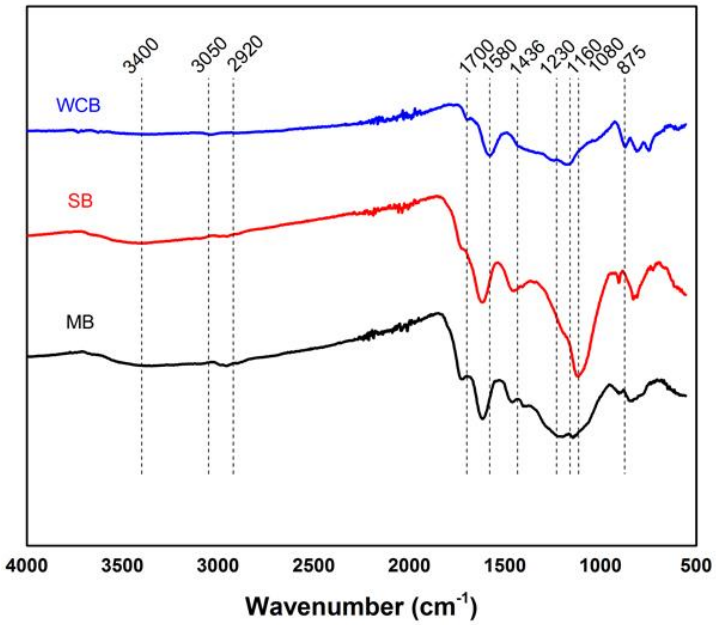


**Fig. 2.** FTIR spectra of biochars

The peak at 875 $cm^{-1}$ represented the out-of-plane deformation produced by aromatic C-H atoms (Tatzber *et al.* 2007). The presence of functional groups such as carboxyl groups could be further utilized for reacting with specific polymers' functional groups or compatibilizers to enhance the compatibility with matrix polymer (Mahmood *et al.* 2013).

The XRD patterns of the biochars are represented in Fig. 3 with the diffracted beam as the intensity and as a function of the Bragg angle (2 theta). Sharp peaks in the SB indicated the presence of various inorganic components, which were related to the crystalline forms of $SiO_2$ and CaO (Kim *et al.* 2011; Liu *et al.* 2012). The present data suggests that most of the crystalline regions present in the biochar come from the cellulose crystallinity and that turbostratic crystallites were very limited in the structure. The WCB exhibited a peak at 43.5 °; however, this was absent in the other biochars. This peak corresponds to the formation of turbostratic carbon crystallites within the biochar's structure (Kim *et al.* 2011). Compared to the XRD peaks of synthetic graphite (Bourke *et al.* 2007), all biochars consisted of broad and featureless structures. All of the results were consistent with the phase diagram and XRD results presented in the work done by Keiluweit *et al.* (2010).

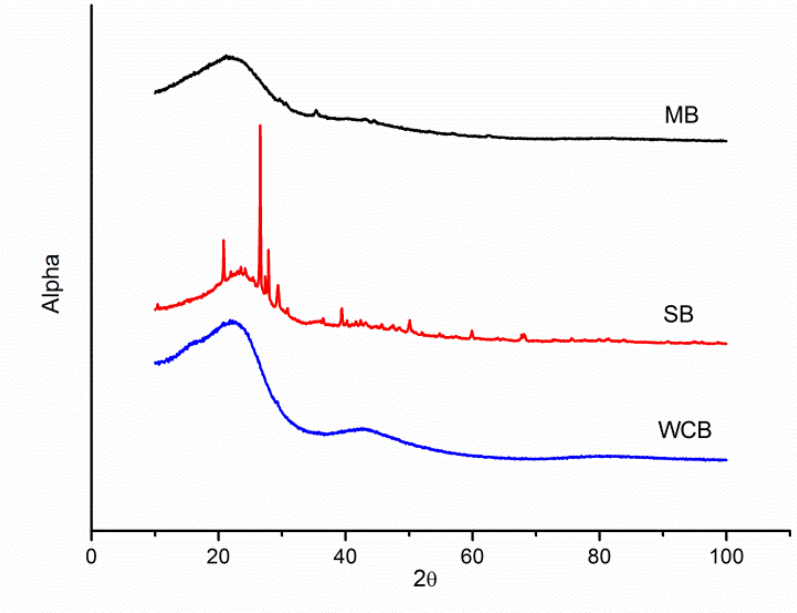


**Fig. 3.** XRD patterns for biochars

The results from the estimation of the particle size distribution, with respect to weight fraction, are shown in Fig. 4. It was observed that the particle size distributions of the milled biochars were mostly within the 0 to 150 µm range, with about 50% below 75 µm range. A significant weight fraction of the WCB was within the particle size range of greater than 500 µm. This was because the dense and hard particles within the wood chips were not easily broken down during the milling process. The porosity of the biochars makes them inherently weak. However, milling can break down the biochar structure from its defective points (pores). Therefore, the resultant particles will be smaller in size and possibly with fewer defects.

Water adsorption of the biochars was highly dependent on the surface properties of the particles: surface area, pore volume and size, oxygenated groups, carbon content, *etc*. High surface area, pore volume, and pore size generally results in a higher moisture uptake,

while the lack of oxygenated groups may reduce the uptake significantly. This is because the affinity between oxygenated groups and water molecules occurs through hydrogen bonding (Brennan *et al.* 2002).

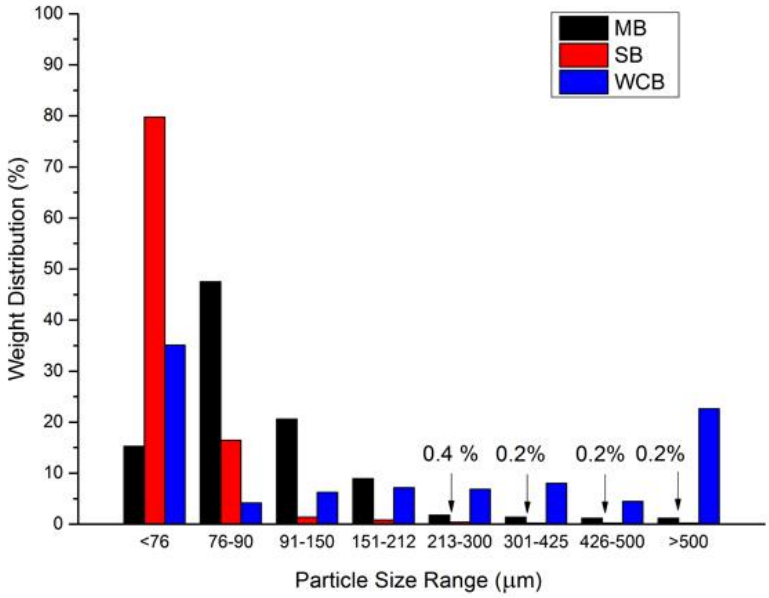


**Fig. 4.** Particle size distribution of biochars

The moisture adsorption of the biochars (Fig. 5) shows that the SB exhibited the highest uptake, while the MB and WCB were relatively comparable. It was expected that the WCB would exhibit the highest moisture content because of its surface area, which was approximately 10 to 15 times greater than SB and MB. This behavior could be attributed to the combined effect of surface area, pore blocking, and oxygenated groups of the biochars (Brennan *et al.* 2002).

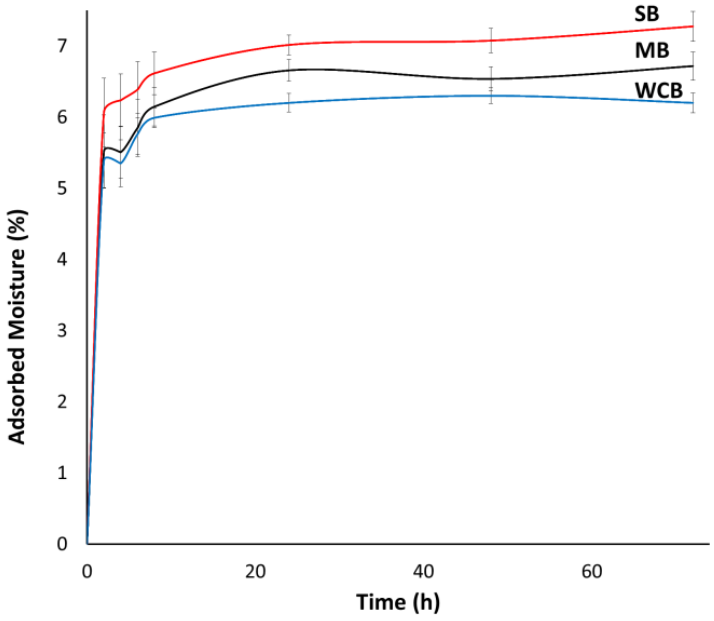


**Fig. 5.** Moisture absorption behavior of biochars

As water molecules come in contact with the surface of the biochars, they first bond to the existing surface oxygenated groups through hydrogen bonding. The amount of carbon, oxygen, hydrogen, and their atomic ratios (Table 1) suggest that the SB and MB contained more oxygenated groups than the WCB. This could have significantly increased the moisture uptake behavior of the SB and MB surfaces. The BET measurement (Fig. 1) suggested that the WCB had a micro-porous structure (pores with an opening less than 20 Å) within its observable macro pores, while the SB and MB had a macro-porous structure (pores with openings exceeding 500 Å) with very small amount of micro-porosity. This can be understood by observing the pore size distribution graphs shown in Fig. 6. It can be observed that the majority of pores in WCB had diameters below 20 Å, while those of SB and MB were bigger than 35 Å. The water molecules of SG and MB were able to freely penetrate into the structure because of the macro-pore size, while in the case of WCB, the micro-pores could easily be blocked or clogged by the bridging of the water molecules. Bridging of the water molecules resulted from a strong binding affinity. With the water molecules having a cross sectional area of 10.6 Å2/ molecule (Livingston 1944), they could easily block the pores of the WCB, which has a cross sectional area of less than 20 Å.

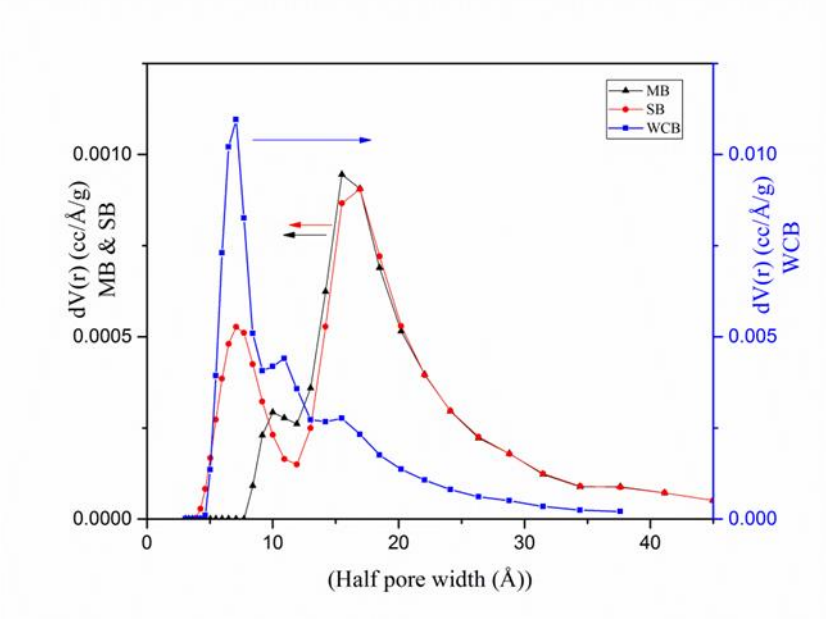


**Fig. 6.** Pore size distribution of biochars

The DMT modulus images of all biochars are shown in Fig. 7. Several images were taken from different sections of the composites and the images are representative of all scanned areas (Fig. 7). Height images showed no differences larger than 800 nm.

Modulus measurement results showed that the wood chip biochar had the highest DMT modulus compared to the other biochars. Table 2 summarizes the modulus values for all four biochars. Moduli of both grass-based biochars were fairly similar, while the wood-based biochar was almost double. This could be related to the higher amount of fixed carbon existing in wood chip biochar sample. These values are higher than the typical Young's modulus of synthetic polymers, and therefore addition of biochar to polymeric matrices would have a reinforcing effect when used alone or as a partial replacement of other filler (Peterson *et al.* 2015). Salak *et al.* (2015) reported that biochar was a better reinforcement compared to its parent biomass when used as a filler in poly lactic acid.

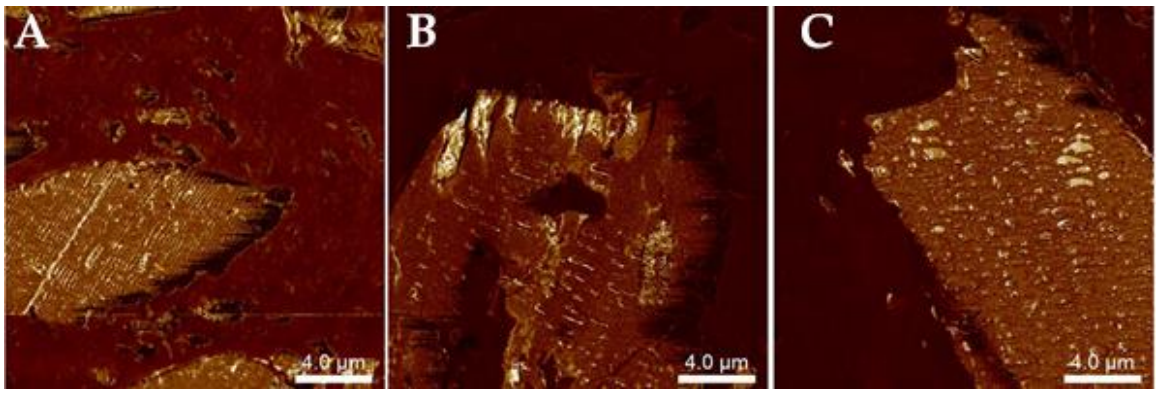


**Fig. 7.** DMT modulus images of A) MB, B) SB, and C) WCB in PP matrix

**Table 2.** Mean DMT Modulus Values for the Biochars

| Samples | DMT Modulus [GPa] |
|---|---|
| Miscanthus Biochar (MB) | 5.03 ± 0.76 |
| Switchgrass Biochar (SB) | 6.26 ± 1.43 |
| Wood Chip Biochar (WCB) | 10.66 ± 1.9 |

The ability of the biochars to effectively conduct electricity depends on several factors, such as the packing density of the biochar particles, particle size, surface elements (especially oxygen groups present on the biochar), crystalline structure, and available electrons within their structures (Pantea *et al.* 2001). Biochars produced at temperatures below 500 °C typically have less aromatic structures, and therefore have fewer available electrons for conducting electricity (Keiluweit *et al.* 2010). Furthermore, the XRD analysis showed the undeveloped crystalline structure of the biochars. Therefore, biochar, in comparison to carbonized biomass, such as lignin (Snowdon *et al.* 2014), has a much lower electrical and thermal conductivity. From the results of the electrical and thermal conductivity testing, there were no notable differences between the values of the biochars resulting from differences in the surface elements. The electrical and thermal conductivities of the biochars are listed in Table 3.

**Table 3.** Thermal and Electrical Properties of the Biochars

| | Thermal Properties | | | Electrical Property |
|---|---|---|---|---|
| Sample | Conductivity ($W\ m^{-1}\ K^{-1}$) | Diffusivity ($mm^2\ s^{-1}$) | Specific Heat ($MJ\ m^{-3}\ K^{-1}$) | Electrical Conductivity ($Sm^{-1}$) |
| MB | 0.15241 ± 0.00421 | 0.06723 ± 0.00358 | 2.3348 ± 0.0753 | 0.00953 ± 0.00050 |
| SB | 0.15322 ± 0.00615 | 0.05223 ± 0.00477 | 2.2232 ± 0.1063 | 0.00869 ± 0.00015 |
| WCB | 0.17513 ± 0.00574 | 0.06201 ± 0.00508 | 2.9426 ± 0.1437 | 0.00939 ± 0.00006 |

The results of the thermal and electrical conductivity tests were similar. There were marginal differences in the WCB thermal and electrical conductivity that may have been because of its turbostratic structure, observed from the XRD spectra. It was difficult to correlate these results because there were many contributing factors, such as the heterogeneity of particle shapes, particle sizes, porosity, chemical composition, crystallinity, presence of impurities, *etc*.

## CONCLUSIONS

1. The relatively high elastic modulus and availability of surface functional groups indicate that biochars could be promising as the reinforcement of bio-filler for polymer composite applications.
2. The smaller pore size and higher pore volume of wood chip biochar compared to other biochars revealed its benefit for filtration applications.
3. The moisture analysis showed that the pores of WCB were too small for water molecules to be absorbed into its structure. Therefore, the high surface area resulting from its porosity would not be accessible by polymer molecules. The reduction in WCB particle size will allow for further increases in surface area and interaction with polymer chains.
4. Short cycle mechanical milling proved to be an effective method for reducing the WCB particle size.
5. Regardless of the biomass source, a 500 °C pyrolysis temperature does not result in enough crystalline structure to enhance the thermal and electrical conductivities. Hence, an elevated pyrolysis temperature is suggested for applications which require better electrical and thermal properties.

## ACKNOWLEDGMENTS

We gratefully acknowledge the financial support of the Ontario Ministry of Agriculture, Food and Rural Affairs (OMAFRA)/University of Guelph - Bioeconomy for Industrial Uses Research Program Theme Project # 200399 and # 030055; and the Natural Sciences and Engineering Research Council (NSERC), Canada NCE AUTO21 Project # 460372 and 460373 to carry out this research work.

## REFERENCES CITED

Asai, H., Samson, B. K., Stephan, H. M., Songyikhangsuthor, K., Homma, K., Kiyono, Y., Inoue, Y., Shiraiwa, T., and Horie, T. (2009). "Biochar amendment techniques for upland rice production in Northern Laos: 1. Soil physical properties, leaf SPAD and grain yield," *F. Crop. Res*. 111(1-2), 81-84. DOI: 10.1016/j.fcr.2008.10.008

Atkinson, C. J., Fitzgerald, J. D., and Hipps, N. A. (2010). "Potential mechanisms for achieving agricultural benefits from biochar application to temperate soils: A review," *Plant Soil* 337(1-2), 1-18. DOI: 10.1007/s11104-010-0464-5

Bourke, J., Manley-Harris, M., Fushimi, C., Dowaki, K., Nunoura, T., and Antal, M. J. (2007). "Do all carbonized charcoals have the same chemical structure? 2. A model of the chemical structure of carbonized charcoal," *Ind. Eng. Chem. Res*. 46(18), 5954-5967. DOI: 10.1021/ie070415u

Brennan, J. K., Thomson, K. T., and Gubbins, K. E. (2002). "Adsorption of water in activated carbons: effects of pore blocking and connectivity," *Langmuir* 18(14), 5438-5447. DOI: 10.1021/la0118560

Brown, T. R., Wright, M. M., and Brown, R. C. (2011). "Estimating profitability of two biochar production scenarios: A low pyrolysis *vs*. fast pyrolysis," *Biofuels, Bioprod. Biorefin.* 5(1), 54-68. DOI: 10.1002/bbb.254

Caillat, S., and Vakkilainen, E. (2013). "Large-scale biomass combustion plants: An overview," in: *Biomass Combustion Science, Technology and Engineering*, Rosendahl, L. (ed.), Woodhead Publishing, Cambridge. DOI:10.1533/9780857097439.3.189

Cherubini, F. (2010). "The biorefinery concept: Using biomass instead of oil for producing energy and chemicals," *Energy Convers. Manag*. 51(7), 1412-1421. DOI: 10.1016/j.enconman.2010.01.015

Freddo, A., Cai, C., and Reid, B. J. (2012). "Environmental contextualisation of potential toxic elements and polycyclic aromatic hydrocarbons in biochar," *Environ. Pollut*. 171, 18-24. DOI: 10.1016/j.envpol.2012.07.009

Gaskin, J. W., Steiner, C., Harris, K., Das, K. C., and Bibens, B. (2008). "Effect of low-temperature pyrolysis conditions on biochar for agricultural use," *Trans. ASABE* 51(6), 2061-2069. DOI: 10.13031/2013.25409

González, M. E., Cea, M., Sangaletti, N., González, A., Toro, C., Diez, M. C., Moreno, N., Querol, X., and Navia, R. (2013). "Biochar derived from agricultural and forestry residual biomass: Characterization and potential application for enzymes immobilization," *J. Biobased Mater. Bioenergy* 7(6), 724-732. DOI: 10.1166/jbmb.2013.1373

Keiluweit, M., Nico, P. S., Johnson, M. G., and Kleber, M. (2010). "Dynamic molecular structure of plant biomass-derived black carbon (biochar)," *Environ. Sci. Technol*. 44(4), 1247–53. DOI: 10.1021/es9031419

Khan, A., Mirza, M., Fahlman, B., Rybchuk, R., Yang, J., Harfield, D., and Anyia, A. O. (2015). "Mapping thermomechanical pulp sludge (TMPS) biochar characteristics for greenhouse produce safety," *J. Agric. Food Chem.* 63(5), 1648-1657. DOI: 10.1021/jf502556t

Kim, P., Johnson, A., Edmunds, C. W., Radosevich, M., Vogt, F., Rials, T. G., and Labbé, N. (2011). "Surface functionality and carbon structures in lignocellulosic-derived biochars produced by fast pyrolysis," *Energy Fuels* 25(10), 4693-4703. DOI: 10.1021/ef200915s

Koutcheiko, S., and Vorontsov, V. (2013). "Activated carbon derived from wood biochar and its application in supercapacitors," *J. Biobased Mater. Bioenergy* 7(6), 733-740. DOI: 10.1166/jbmb.2013.1375

Laird, D. A., Brown, R. C., Amonette, J. E., and Lehmann, J. (2009). "Review of the pyrolysis platform for coproducing bio-oil and biochar," *Biofuels, Bioprod. Biorefin*. 3(5), 547-562. DOI: 10.1002/bbb.169

Lee, J. W., Kidder, M., Evans, B. R., Paik, S., Buchanan III, A. C., Garten, C. T., and Brown, R. C. (2010). "Characterization of biochars produced from cornstovers for soil amendment," *Environ. Sci. Technol*. 44(20), 7970-7974. DOI:

10.1021/es101337x

Lehmann, J., and Joseph, S. (2009). "Biochar for environmental management: An introduction," in: *Biochar for Environmental Management: Science and Technology*, Lehmann, J., and Joseph, S. (eds.), Routledge, Abingdon, Oxon.

Liu, Y., Zhao, X., Li, J., Ma, D., and Han, R. (2012). "Characterization of bio-char from pyrolysis of wheat straw and its evaluation on methylene blue adsorption," *Desalin. Water Treat.* 46(1-3), 115-123. DOI: 10.1080/19443994.2012.677408

Livingston, H. K. (1944). "Cross-sectional areas of molecules adsorbed on solid surfaces," *J. Am. Chem. Soc.* 66(4), 569-573. DOI: 10.1021/ja01232a021

Lowell, S., Shields, J. E., Thomas, M. A., and Thommes, M. (2004). "Adsorption isotherms," in: *Characterization of Porous Solids and Powders: Surface Area, Pore Size and Density*, Springer, Netherlands, Boston. DOI:10.1007/978-1-4020-2303-3

Mahmood, N., Islam, M., Hameed, A., and Saeed, S. (2013). "Polyamide 6/multiwalled carbon nanotubes nanocomposites with modified morphology and thermal properties," *Polymers* (Basel) 5(4), 1380-1391. DOI: 10.3390/polym5041380

Mohanty, A. K., Misra, M., Rodriguez-Uribe, A., and Vivekanandhan, S. (2015). "Hybrid sustainable composites and methods of making and using thereof,"

Pantea, D., Darmstadt, H., Kaliaguine, S., Sümmchen, L., and Roy, C. (2001). "Electrical conductivity of thermal carbon blacks: Influence of surface chemistry," *Carbon N. Y.* 39(8), 1147-1158. DOI: 10.1016/S0008-6223(00)00239-6

Peterson, S. C. (2012). "Utilization of low-ash biochar to partially replace carbon black in styrene-butadiene rubber composites," *J. Elastomers Plast.* 45(5), 487-497. DOI: 10.1177/0095244312459181

Peterson, S. C., Chandrasekaran, S. R., and Sharma, B. K. (2015). "Birchwood biochar as partial carbon black replacement in styrene-butadiene rubber composites," *J. Elastomers Plast.* DOI: 10.1177/0095244315576241

Peterson, S. C., Jackson, M. A., Kim, S., and Palmquist, D. E. (2012). "Increasing biochar surface area: Optimization of ball milling parameters," *Powder Technol.* 228, 115-120. DOI: 10.1016/j.powtec.2012.05.005

Salak, F., Uemura, S., and Sugimoto, K. (2015). "Thermal pretreatment of kudzu biomass (*Pueraria lobata*) as filler in cost-effective PLA biocomposite fabrication process," *Polym. Eng. Sci.* 55(2), 340-348. DOI: 10.1002/pen.23909

Sarmah, A. K., Srinivasan, P., Smernik, R. J., Manley-Harris, M., Antal, M. J., Downie, A., and van Zwieten, L. (2010). "Retention capacity of biochar-amended New Zealand dairy farm soil for an estrogenic steroid hormone and its primary metabolite," *Aust. J. Soil Res.* 48(7), 648. DOI: 10.1071/SR10013

Schwanninger, M., Rodrigues, J. C., Pereira, H., and Hinterstoisser, B. (2004). "Effects of short-time vibratory ball milling on the shape of FT-IR spectra of wood and cellulose," *Vib. Spectrosc.* 36(1), 23-40. DOI: 10.1016/j.vibspec.2004.02.003

Shackley, S., Sohi, S., Ibarrola, R., Hammond, J., Masek, O., Brownsort, P., Cross, A., Prendergast-Miller, M., and Haszeldine, S. (2013). "Biochar, tool for climate change mitigation and soil management," in: *Geoengineering Responses to Climate Change SE - 6*, Lenton, T., and Vaughan, N. (eds.), Springer, New York. DOI:10.1007/978-1-4614-5770-1_6

Smidt, E., and Meissl, K. (2007). "The applicability of Fourier transform infrared (FT-IR) spectroscopy in waste management," *Waste Manag.* 27(2), 268-276. DOI: 10.1016/j.wasman.2006.01.016

Snowdon, M. R., Mohanty, A. K., and Misra, M. (2014). "A study of carbonized lignin as

an alternative to carbon black," *ACS Sustain. Chem. Eng*. 2(5), 1257-1263. DOI: 10.1021/sc500086v

Spokas, K. A., Koskinen, W. C., Baker, J. M., and Reicosky, D. C. (2009). "Impacts of woodchip biochar additions on greenhouse gas production and sorption/degradation of two herbicides in a Minnesota soil," *Chemosphere* 77(4), 574-581. DOI: 10.1016/j.chemosphere.2009.06.053

Stuart, B. H. (2004). *Infrared Spectroscopy: Fundamentals and Applications*, John Wiley & Sons, Ltd, Chichester, UK

Tanger, P., Field, J. L., Jahn, C. E., Defoort, M. W., and Leach, J. E. (2013). "Biomass for thermochemical conversion: targets and challenges," *Front. Plant Sci*. 4(July), 218. DOI: 10.3389/fpls.2013.00218

Tatzber, M., Stemmer, M., Spiegel, H., Katzlberger, C., Haberhauer, G., Mentler, A., and Gerzabek, M. H. (2007). "FTIR-spectroscopic characterization of humic acids and humin fractions obtained by advanced NaOH, $Na_4P_2O_7$, and $Na_2CO_3$ extraction procedures," *J. Plant Nutr. Soil Sci*. 170(4), 522-529. DOI: 10.1002/jpln.200622082

Tumuluru, J. S., Boardman, R. D., Wright, C. T., and Hess, J. R. (2012). "Some chemical compositional changes in miscanthus and white oak sawdust samples during torrefaction," *Energies* 5(10), 3928-3947. DOI: 10.3390/en5103928

Van Zwieten, L., Kimber, S., Morris, S., Chan, K. Y., Downie, A., Rust, J., Joseph, S., and Cowie, A. (2009). "Effects of biochar from slow pyrolysis of papermill waste on agronomic performance and soil fertility," *Plant Soil* 327(1-2), 235-246. DOI: 10.1007/s11104-009-0050-x

Walters, R. C., Fini, E. H., and Abu-lebdeh, T. (2014). "Enhancing asphalt rheological behavior and aging susceptibility using bio-char and nano-clay," *Am. J. Eng. Appl. Sci.* 7(1), 66-76. DOI: 10.3844/ajeassp.2014.66.76

Warnock, D. D., Lehmann, J., Kuyper, T. W., and Rillig, M. C. (2007). "Mycorrhizal responses to biochar in soil – concepts and mechanisms," *Plant Soil* 300(1-2), 9-20. DOI: 10.1007/s11104-007-9391-5

Yao, Y., Gao, B., Chen, J., Zhang, M., Inyang, M., Li, Y., Alva, A., and Yang, L. (2013). "Engineered carbon (biochar) prepared by direct pyrolysis of Mg-accumulated tomato tissues: characterization and phosphate removal potential," *Bioresour. Technol*. 138, 8-13. DOI: 10.1016/j.biortech.2013.03.057

Yu, J. T., Dehkhoda, A. M., and Ellis, N. (2011). "Development of biochar-based catalyst for transesterification of canola oil," *Energy Fuels* 25(1), 337-344. DOI: 10.1021/ef100977d

Article submitted: June 25, 2015; Peer review completed: October 2, 2015; Responses to reviewer comments received and approved: November 7, 2015; Revised version received and accepted: November 9, 2015; Published: December 15, 2015.
DOI: 10.15376/biores.11.1.1334-1348